WINDWARD-SIDE OROGRAPHIC EFFECTS OF THE SUBTROPICAL AND EXTRATROPICAL ANDES ON PRECIPITATING CLOUDS

Maximiliano Viale and René Garreaud
maxiviale@yahoo.com.ar
Departamento de Geofísica, Facultad de Ciencias Físicas y Matemáticas,
Universidad de Chile, Santiago, Chile.

RESUMEN

El efecto orográfico de la cordillera de los Andes (30°S-55°S) sobre las nubes precipitantes a barlovento es investigado a partir de datos de superficie y satelitales. Datos de precipitación en superficie entre los 33ºS y 44ºS, indican que la precipitación anual aumenta desde la costa del Pacifico hasta el sector pendiente arriba de la cordillera por un factor de 1.6 ± 0.2. Mediciones horarias de superficie e instantáneas de satélites revelan que el incremento orográfico de la precipitación anual responde a un incremento de la intensidad y la frecuencia de la precipitación hacia la cordillera. El efecto orográfico sobre las nubes precipitantes es más acentuado en latitudes subtropicales (30°S-40°S) que en latitudes extratropicales (40°S-55°S) según los datos satelitales CloudSat. Al sur de los 40ºS, la profundidad de las nubes decrece débilmente desde el océano a los Andes. El contenido total de hielo en las nubes prácticamente no cambia desde el océano a los Andes, pero el contenido máximo de hielo en las nubes ubicadas en el sector pendiente arriba de los Andes es mayor y ocurre en niveles más bajos que los observados en las nubes sobre el océano. Estos resultados sugieren que las partículas de hielo en la parte alta de las nubes son producidas por mecanismos de ascensos de escala sinóptica, mientras que mecanismos de ascensos orográficos en niveles bajos aceleran el crecimiento de gotas por procesos de riming y su posterior caída sobre los Andes extratropicales. Al norte de los 40ºS, las nubes sobre los océanos son chatas y prácticamente no contienen hielo. El contenido total y máximo de hielo se incrementa considerablemente en las nubes sobre los altos Andes subtropicales, con valores mucho más altos que su contraparte sobre los Andes extratropicales. Además, el incremento de hielo en las nubes comienza antes de la cordillera, probablemente debido a un bloqueo orográfico del flujo del oeste en niveles bajos.

ABSTRACT

The orographic effect of the Andes (30°S-55°S) on windward-side precipitating clouds from mid-latitude frontal systems is investigated using surface and satellite data. Rain gauges between 33°S and 44°S indicate that annual precipitation increases from the Pacific coast to the windward slopes by a factor of 1.6 ± 0.2. Hourly gauges and instantaneous satellite estimates reveal that the cross-barrier increase in annual precipitation responds to an increase in both the intensity and frequency of rainy events. Orographic effects of the Andes are stronger at subtropical (30°S-40°S) than at extratropical latitudes (40°S-55°S) according to CloudSat satellite data. To the south of 40°S, the depth of the cloud layer slightly decreases from offshore to the Andes. The total ice content changes little in the cross-mountain direction, but the maximum ice content over the windward slopes is larger and occurs at a lower level than its counterpart offshore. These results suggest that ice particles aloft are produced by synoptic-scale ascent but low-level orographic lifting accentuate the riming process, thus accelerating the particles growth and fall out over the extratropical Andes. At subtropical latitudes, the clouds over the ocean are shallow and contain minimal ice aloft. The total and maximum ice content significantly increases toward the tall subtropical Andes, with values being much higher than their counterparts over the extratropical Andes. Further, the increase in ice content starts before the barrier, likely as a result of upstream blocking.

Key words: Andes cordillera, orographic effects, midlatitudes precipitating cloud properties.

1) INTRODUCTION

Frontal precipitation systems rooted in midlatitude cyclones are profoundly altered when moving over major mountain ranges (e.g., *Houze*, 2012), often producing orographic precipitation enhancement over the windward slopes of the mountains and a rain shadow to their lee. Orographic effects of the subtropical Andes on frontal precipitation have been more explored than those of the extratropical Andes. Climatological approaches using surface and rawinsonde observations have documented a precipitation enhancement over the relatively dry (<1000 mm/year) windward slopes of the subtropical Andes during the passage of cold fronts (*Falvey and Garreaud*, 2007; *Viale and Nuñez*, 2011). Further airflow analyses from case studies revealed that blocked low-level poleward winds intensifies convergence on the equatorward moving front (*Barrett et al.*, 2009) forcing the midlevel westerly flow to rise before the mountain barrier. The forced uplift produces a midlevel layer cloud deck with ice particles, which in turn, interact with the approaching front and enhance precipitation upstream of the barrier (*Viale et al.*, 2013).

The extratropical Andes locate in the remote Patagonia region, where their upstream sector features inaccessible islands and sparsely populated terrain with virtually nonexistent surface stations. Mean annual precipitation in this sector is above 3000 mm. Understandably, the few existent climatological approaches to orographic precipitation in the southern Andes has been based on long-term numerical simulation (*Garreaud et al.*, 2013; *Lenaerts et al.*, 2014) or on indirect estimates, such as stable isotope data from streamwater (*Smith and Evans*, 2007) or lightining activity data (*Garreaud et al.*, 2014). Nonetheless, there is clear evidence for a marked precipitation enhancement to the west of the extratropical Andes.

In the present study we aim at characterizing the upstream orographic effects of the Andes (south of 30°S) by using surface and CloudSat satellite observations (see details in section 2). Raingauges with daily and hourly records allow a first order estimation of the rainfall increase from the coast towards the mountains at different latitudes (section 3). The multiyear satellite dataset is then used to characterize macro- and micro-physical properties of precipitating clouds upstream of the subtropical and extratropical Andes (section 4) helping to interpret the surface observations and compare the orographic effects in the two different sectors of the Andes (semi-arid and high versus hyper-humid and low). Discussion and main results are summarized and in section 5.

2) DATA AND METHODOLOGY

Figure 1a shows the location of the precipitation stations used in this study superimposed on a topographic map of the west coast of southern South America. Two types of datasets are available. The daily precipitation (recorded at 1200 UTC) dataset from DGA-Chile consists of 216 stations located between 33º and 44ºS over a 10-year record (2002-2011). The hourly precipitation dataset consists of 47 automatic stations, 35 of them managed by AGROMET-Chile and 12 of them installed by the authors, covering from April 2013 to August 2014. Because the AGROMET stations locate mostly on the central valley west of the Andes, we installed our stations in five east-west transects (at 36°S, 38°, 40°, 42°, and 44°S) from the coast to the upslope sector of the Andes. For both datasets, we retained stations with less than 10% of missing values and located below 2000 m, since the rain gauges were not suited to measure snow.

To characterize properties of precipitating cloud, we use CloudSat and CALIPSO satellite data. Unlike the surface precipitation data, the satellite products extend over the entire extratropical range allowing a comparison between the clouds systems upstream of the subtropical and extratropical Andes. CloudSat has a Cloud Profiling Radar sensor (CPR, Im et al. (2005)) that is sensitive to cloud

and precipitation particles; CALIPSO has a cloud-aerosol lidar sensor (CALIOP, Winker et al. (2009)) and is more sensitive to thin clouds that could be missed by CPR. The two satellites orbit since 2006 (CALIPSO stop its measurements in 2011) in NASA's A-Train constellation in a polar orbit (Stephens et al., 2002) enabling the overlap of the radar and lidar footprints. The horizontal resolution of the footprint is 1.7 km (cross track) by 1.3 km (along track), and the profiles has 125 vertical bins of 240 m thick from the surface to near 30 km height. More than seven years (2007-2014) of CloudSat radar only data and almost four years (2006-2011) of CloudSat-CALIPSO combined radar-lidar data were analyzed over the west coast of South America. For the purpose of this study, only rainy vertical profiles were analyzed. Insight of the macro- and micro-physical properties of precipitating clouds were gained by analyzing the base and top heights of the cloud layers, as well as the ice content parameters available in the 2B-GEOPROF-LIDAR (Mace et al., 2009) and the 2B-CWR-RO (Austin et al., 2009) products, respectively.

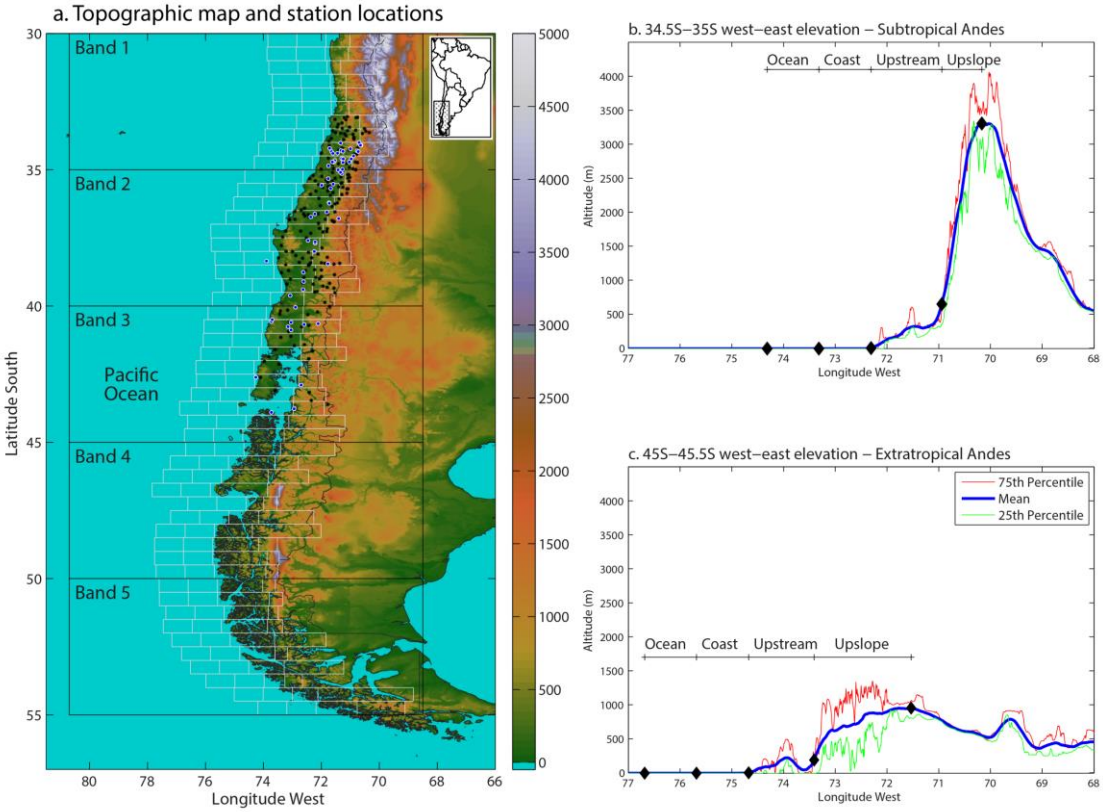

Figure 1: (a) The study region over the west coast of the southern South America with the daily (asterix) and hourly (circle) rain-gauges datasets. To illustrate the criterion used to define the Ocean, coast, upstream, and upslope cross-barrier zones within 0.5°-width (white rectangles), two meridionally averaged east-west elevation of the Andes (blue line) and 25th and 75th percentile altitude (green and red lines) are presented for the (b) 35°-34.5°S and the (c) 45°-45.5°S latitudinal bands, representative of the subtropical and extratropical Andes, respectively. The black rectangles represent the 5°-width latitudinal bands used for grouping vertical profiles from the CloudSat dataset.

To examine the first-order upstream influence of the Andes we considered a sequence of zonal transects extending from the Pacific Ocean to the Andes ridge. The transects do not overlap, have a width of 0.5° of latitude and cover from 30°S to 55°S (Fig. 1). In each transect we calculate the meridional average of the elevation of the Andes and find the longitude and altitude of the crest (highest point). We then subdivide each transect in four cross-barrier zones from the crest of the Andes to the open Ocean (Fig. 1b-c): upslope, upstream, coastal and ocean. The upslope zone extends from the crest to the (western) foothill, defined as the point with height equal to a quarter of the crest within

each transect. The upstream zone extends from the foothill to the coastline, thus including the low terrain where most of Chilean cities are located. The coastal and Ocean zones are the successive parts of the transect extending westward 0-100 and 100-200 km over the Pacific, respectively.

Each surface station and satellite-based profile were grouped according to its cross-barrier and latitudinal location, using the four zones defined above. When analyzing the satellite profiles, we grouped the 0.5° latitude transects in five latitudinal bands of 5° each to ensure a good sample size to calculate statistics (i.e., in the area enclosed by black rectangles in Fig. 1a). The number of satellite-based profiles available over each zone ranged from 60000 to 130000 over the whole period (2007-2014), from which around 35% and 5% classified as rainy profiles in the southernmost and northernmost latitude bands, respectively.

3) OROGRAPHIC EFFECTS ON PRECIPITATION AS SEEN BY SURFACE DATA

In this section, we focus on the cross-barrier variation in precipitation, considering either daily or hourly data for the annual mean accumulation (R_m), frequency (R_f) and intensity (R_i).
Figure 2 shows the annual mean rainfall accumulation in zonal transects of 1° of latitude each. The stations are differentiated according to their location in the upstream or upslope zones following the procedure described in section 2.3. The orographic enhancement of Rm over the western side of the Andes is evident in all sampled transects of R_m (and extremes of R_m). Considering the Andes between 33°S to 44°S, the mean orographic enhancement ratio results 1.56 ± 0.24. The ratios over the subtropical Andes are in agreement with previous observational studies in that region (Falvey and Garreaud, 2007; Viale and Nuñez, 2011).

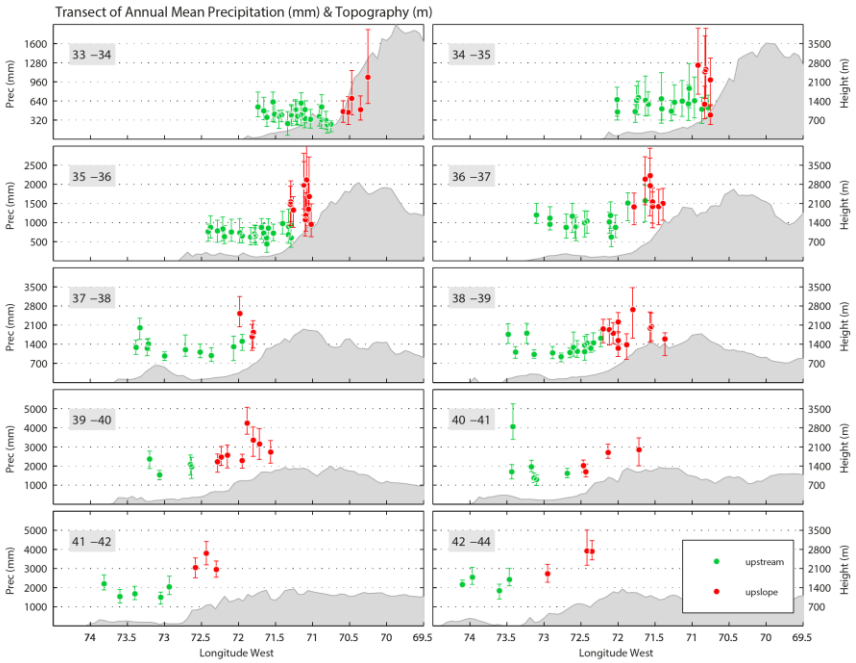

Figure 2: Transect of annual mean precipitation (R_m in mm) from the upstream to the upslope zone. The transects are 1° latitude width (except for the 42°-44° transect due to data availability) and extends from the 33°S to the 44°S, where surface data were available. The circles correspond to the 2002-2011 mean values and the bars to the minimum and maximum annual mean over the 10 year period. The mean east-west altitude (m) is also shown by a gray area plot using GEOTOPO30 data. See text for the definition of the limits to the different cross-barrier zones (upstream, upslope).

A noteworthy aspect of this analysis is that the orographic enhancement –as per the upslope to upstream ratio– does not change significantly from the subtropical Andes to the extratropical Andes, in

spite of the significant change in mean height of the Cordillera (and annual mean accumulation) from ~5000 m ASL (~300 mm) at 33°S to less than 1500 m ASL (~2000 mm) at 44°S. These ratios, however, must be taken with caution due to the low number of stations (especially in the upslope zone), the presence of other topographic features and deviations from the two-dimensional orientation of the Andes. For example, the large ratio observed in the 35°-36°S latitudinal band and the low ratios observed between 38°S and 41°S could be related to an slightly change in the north-south orientation of the Andes cordillera and an elevated coastal range (up to 1000 m ASL), respectively. A denser gauge network and advanced methods for grouping gauges (e.g., Daly et al., 1994; Castro et al., 2014) are needed to better represent spatial distribution of precipitation over complex terrain.

The cross-barrier variation in hourly intensity (median and 25th and 75th percentiles limits of Ri, mm/hr) and frequency (R_f, expressed in %) is displayed in Fig. 3. The number of rainguages available for this analysis is substantially reduced so we considered zonal transects of 2° of latitude. In all transects R_f, as well as the median and 25th and 75th percentile values of R_i, are higher in the easternmost (upslope) stations than those in the westernmost stations (near the coastline). The frequency of hourly rainy events increases from the westernmost to the easternmost station in a factor of between 4% and 10%. The frequency of rainy days exhibits no increase toward the mountains (not shown), so the increase in hourly R_f indicates that sub-daily rainy events over the upslope zone tend to last longer than those over the upstream and costal zones (due to an earlier onset or later demise). The increase in rain frequency from the Pacific Ocean to the upslope zone is corroborated by the instantaneous estimates from the CloudSat data (Table I), which additionally suggest that the increase in Rf over the Andes' windward side is more accentuated between 30°S-45°S than farther south (45°S-55°S). Likewise, the median of R_i increases between 0.1 mm/h and 0.6 mm/h from the westernmost to the easternmost station. Indeed, when considering all the stations in each transect the cross-barrier variation of R_f and R_i is disperse, but the easternmost station in the upsolpe zone always exhibits the largest values. Therefore, the orographic enhancement of precipitation amount along the Andes results from both higher precipitation frequency and intensity over the mountains relative to their counterparts at lower elevations.

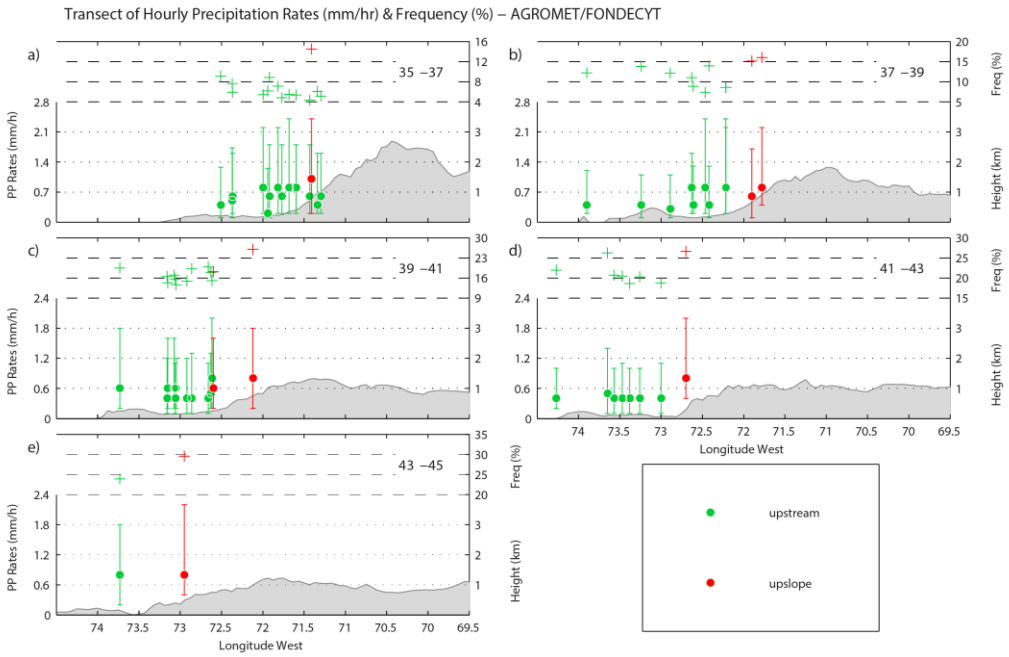

Figure 3: Transects of intensity (R_i circles and barbs in mm h^{-1}) and frequency (R_f - cross in %) of precipitation using hourly rain-gauges dataset for different cross-barrier zones from the upstream (green) to the upslope zone (red). The intensity of precipitation is presented by errorbars with the median (circles) and 25th and 75th percentile limits (barbs) values. The transects are 2° latitude width and extends from the 35°S to the 45°S.

Latitudinal Band	Frequency (%) of rainy profiles from CloudSat satellite data over each cross-barrier zone			
	Ocean	Costal	Upstream	Upslope
30°- 35° S	12%	5%	8%	32%
35°- 40° S	20%	20%	21%	29%
40°- 45° S	32%	38%	38%	46%
45°- 50° S	41%	40%	49%	47%
50°- 55° S	42%	47%	49%	48%

Table I: Frequency (%) of rainy profiles observed by CloudSat satellite data for different cross-barrier zones and different latitudinal bands over the 2007-2014 period.

4) OROGRAPHIC EFFECTS ON RAINY CLOUDS AS SEEN BY SATELLITE DATA

Macrophysical properties of precipitating clouds are analyzed first in Figure 4, which shows the height of cloud base and cloud top in each zone (Ocean, coastal, upstream and upslope) within the 5° of latitude zonal bands (see Fig. 1). In all of these bands, the cloud base height increases from the Ocean to the upslope zone, gradually at midlatitudes and more sharply in the subtropics, somewhat following the topographic profile. The cross-barrier behavior of the cloud top height has more dependence on latitude. To the south of 40°S there is a slight decrease in the cloud top toward the mountains resulting in somewhat thinner clouds layer just over the mountains. Even there, the cloud depth is > 5 km and largely cold as the freezing level at midlatitudes ranges from 1 to 2 km when precipitation occurs (not shown). In contrast, to the north of 40°S the cloud top height increases toward the mountains. The lowest and thinnest precipitating clouds (depth < 3 km) are observed over the ocean zone (100 km offshore), likely as a result of an increasingly influence of the southeast Pacific anticyclone. The freezing level at subtropical latitudes is about 2.5 km so the cloud are largely cold over the continental upstream and upslope zones, while warm rain processes must dominate the offshore clouds.

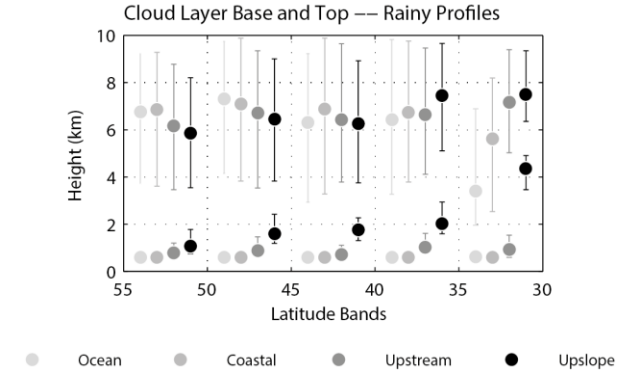

Figure 4: CloudSat 2B-GEOPROF-LIDAR product showing the median values and the the 25th and 75th percentile of the base and top of clouds for different latitude bands and cross-barrier zones.

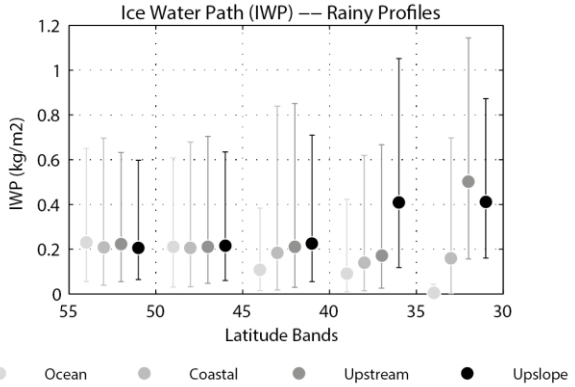

Figure 5: Ice Water Path (IWP in g m^{-2}) for the 5°-width latitudinal bands and the different cross-barrier zones (light gray to black means from the Ocean zone to the upslope zone). The circles correspond to the median values and the bars to the 25th and 75th percentile limits.

Since the primary process of the midlatitudes precipitation systems are of the stratiform type within nimbustratus clouds, where the ice particles grow aloft by vapor diffusion, aggregation, and

riming, and then precipitate producing rain (or snow) on the sufrace (e.g., Houze, 1993), we focus on describing cross-barrier propierties of Ice Water Content (IWC) and its vertical integral (Ice Water Path, IWP) within the rainy clouds. Indeed, observational studies using CloudSat data have recently quantified that cold rain process dominates in frontal systems over the Northeastern Pacific Ocean, especially to north of 40°N, and also produces higher rain rates than warm rain process (Matrosov, 2013). Moreover, warm stratiform clouds (tops below 0°C isotherm) produce light rain and are only relevant over the subtropical offshore zones.

Figure 5 shows the median, 25th and 75th percentile of the IWP when rain is present for the cross-barrier zones within each of 5° of latitude zonal bands (see Fig. 1). To the south of the 45°S, the ice content change little from open Ocean to the upslope of the Austral Andes. In contrast, to the north of 40°S there is a marked increase in IWP from the Ocean to the Andes. Also note that the IWP over the upslope of the subtropical Andes is twice as large as its counterpart over the extratropical Andes.
Further microphysical information is gained from the vertical profiles of IW C for the different cross-barrier zones within the 5° of latitude zonal bands (Figs. 6 and 7). Each profile represents the median values of IWC for in-cloud-portions of 250 m deep. To the south of 40°S, the maximum IWC over the upslope zone is larger than the maximum offshore but, as commented before, the cloud becomes thinner toward the mountains (Fig. 6a-c) so IWP varies little in the cross-barrier direction. Also note that the level of maximum IWC moves downward as one moves towards the mountain, indicative of an augmented density or size of the ice particles just above the freezing level. To the north of 40°S (Fig. 6d-e), there is little ice over the Ocean zone (indicative of warm rain processes), and too much over the Andes. In the transect 30°-35°S (highest Andean elevation), the continental upstream IWC profile is very similar to the profile over the upslope (Fig. 6e), denoting an orographic effect on precipitating clouds that starts before the windward slope of the Andes.

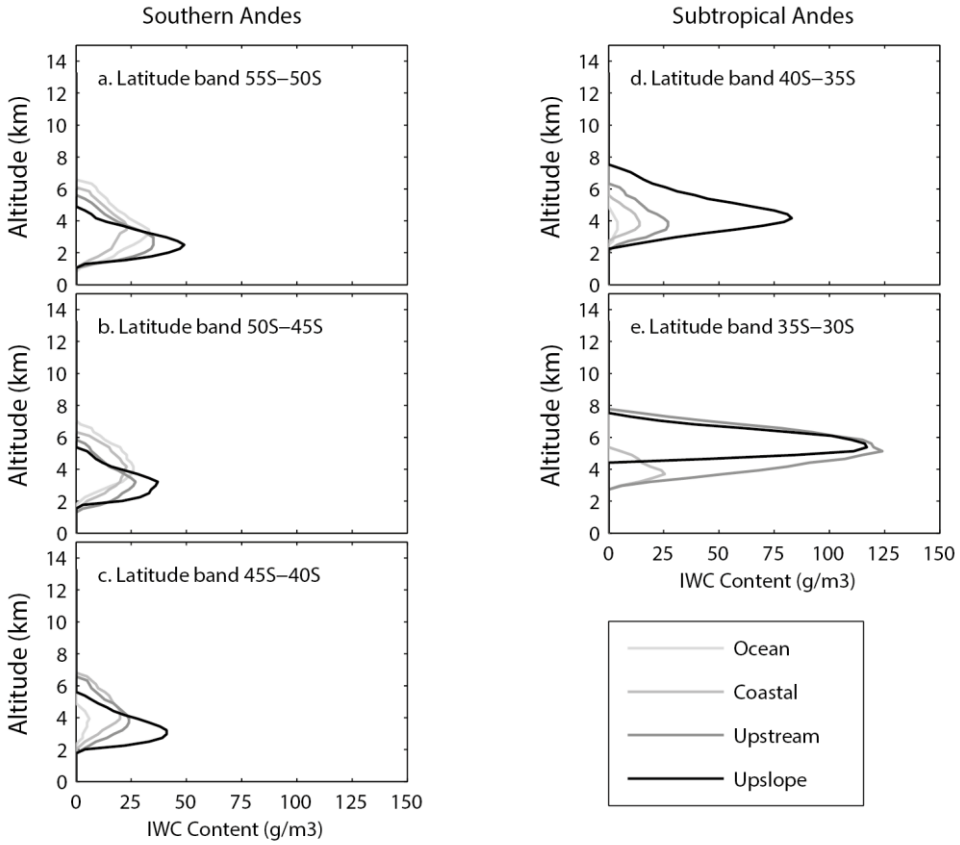

Figure 6: Vertical profiles of Ice Water Content (IWC in g m^{-3}) for different 5°-width latitudinal bands: (a) 55°-50°S, (b)

50°-45°S, (c) 45°-40°S, (d) 40°-35°S, and (e) 35°-30°S. The different colors denote the different cross-barrier zones (light gray to black means from the Ocean to the upslope zones). The vertical profiles show the median values of IWC at each vertical level for only the profiles classified as rainy according to the 2C-PRECIP CloudSat product.

The vertical section of IWC in along-barrier direction (Fig. 7) further illustrates a more accentuated upstream orographic effect of the subtropical Andes than that of the extratropical Andes on increasing ice content within clouds. The IWC maximum over the windward slopes of the subtropical Andes (~70-120 g m^{-3}) is quite higher than its counterpart over the extratropical Andes (~40 g m^{-3}). Conversely, the IWC maximum over the subtropical Ocean (~0 g m^{-3}) is lower than its counterpart over the extratropical Ocean (~30 g m^{-3}).

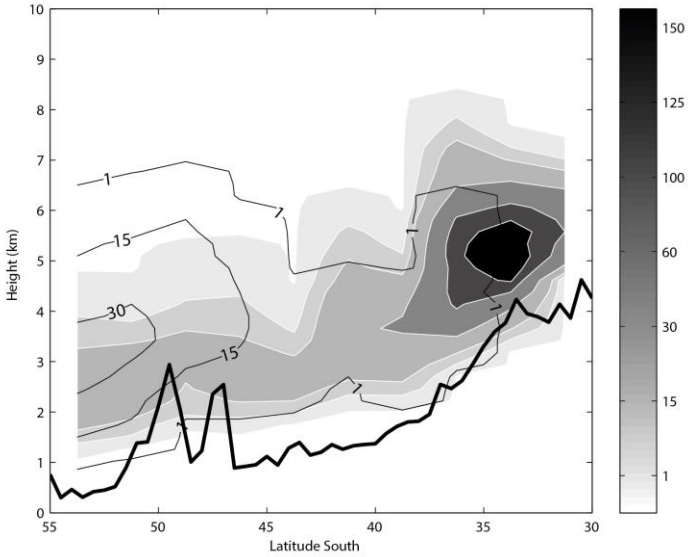

Figure 7: Vertical section in along-barrier direction showing the median values of Ice Water Content (IWC) of rainy profiles from the CWC-RO CloudSat data over the Ocean (lines) and the upslope (shaded) cross-barrier zones. For the definition of Ocean and upslope cross-barrier zones see text. Black thick line shows the crest altitude of the Andes averaged within 0.5°-width latitude band (see Fig. 1). IWC lines contour of 1, 15, 30, 60, 100, 125, and 150 g m-3 are plotted, when are present, for both cross-barrier zones.

5) DISCUSSION AND CONCLUSION

Stratiform precipitation from midlatitude frontal systems falls over the western coast of extratropical South America (year round to the south of 40°S and mostly in austral winter at subtropical latitudes) being profoundly altered as they move over the elevated terrain of the Andes. The upstream orographic effects of the subtropical (30°S-40°S) and extratropical (40°S-55°S) Andes on rainfall and precipitating clouds has been investigated using surface rain gauge and CloudSat satellite data. Recall that the Andes mean height decreases from about 5000 m ASL at subtropical latitudes to less than 1500 m ASL to the south of 40°S.

The annual mean precipitation along the Andes foothills increases from ~300-500 mm at subtropical latitudes to >2000 mm to the south of 40°S, largely a consequence of an increased number of rainy days towards the south. Superimposed in that marked latitudinal variation, the annual mean precipitation increases from the low upstream terrain to the windward slope of the Andes by a factor between 1.2 and 1.8. In spite of the low station density and the existence of other topographic features, the long-term precipitation ratios indicate a consistent Andean orographic enhancement in all sampled latitudes (from 33°S to 44°S), in agreement with previous observational studies in the subtropical region (Falvey and Garreaud, 2007; Viale and Nuñez, 2011). The hourly precipitation data and the instantaneous satellite estimates indicate that the orographic enhancement of the annual precipitation responds to a cross-barrier increase of both the intensity and frequency of rainy events. At any given

zonal transect, the increased frequency of hourly rainy events over the higher terrain is mostly consequence of longer sub-daily rainstorms.

The CloudSat satellite data suggest that the orographic effects on precipitating clouds are more accentuated upstream of the subtropical Andes than upstream of the extratropical Andes, a result attributed to the higher altitude of the subtropical barrier. The main results are summarized as follow. Upstream of the extratropical Andes (40°S-55°S), the total ice content within the precipitating clouds changes little from the open Ocean to the Andes, suggesting that it is primary determined by the synoptic-scale forcing. Nonetheless, the maximum ice content in the vertical profile over the windward slopes is much larger (and occurs at lower levels) than its offshore counterpart. These results suggest that riming becomes more active just above the freezing level as a result of low-level orographic lifting over the windward slopes, which then accelerate the particles growth and fall out over the higher terrain. Overall, greater precipitation efficiency instigated by localized and intense orographic uplift is suggested as the leading mechanism for precipitation enhancement over the southern Andes.

At subtropical latitudes (30°S-40°S), shallow, warm clouds with little precipitation dominate the offshore sector. The westerly winds are largely blocked by the very tall subtropical Andes (e.g., Barret et al., 2009), so the orographically forced ascent begins well before the mountain and encompasses a thick layer (> 4 km) leading to a rapid increase in ice content within midlevel clouds over the upstream zone, and finally to the precipitation enhancement toward the mountains. These results, obtained from a climatological approach, are in line with those from a previous case study of heavy precipitation upstream of the subtropical Andes **(**Viale et al., 2013), which propose possible physical mechanisms. The case study showed through numerical simulation that ice content is orographically increased within prefrontal midlevel clouds, which in turn, interacts with orographically invigorated updrafts on the frontal surface by upstream blocking and enhanced low-level convergence. As a result, a seeder-feeder mechanism becomes active leading to higher ice content within clouds and precipitation rates just upstream of the Andes, compared with those over the open Ocean.

Key questions concerning the physical mechanism operating in the orographic precipitation arise from the present climatological study and should be addressed in future works, especially over the austral Andes (45°S-55°S) where the lack of surface stations has precluded an estimation of the orographic enhancement in an extremely rainy environment (>5000 mm/year). Comparative cases study over the extratropical and subtropical Andes using numerical simulations, dedicated in-situ observations and satellite data could be the next step, in order to gain further insight into the mesoscale airflow dynamics and orographic precipitation processes over both sectors of the Andes.

Acknowledgments: This research was supported by FONDECYT 3130688 and FONDAP CR2. CloudSat data were obtained from the CloudSat Data Processing Center (cloudsat.cira.colostate.edu). Rain gauges data were obtained from the Red Agroclimatica Nacional (AGROMET) and Dirección General de Aguas (DGA) de Chile. We are very grateful to El Chacay and Andean Rose lodgings, Carabineros de Chile, INDAP-Chaiten, staff of the Chilean National Park (CONAF) in Cucao and Mocha Island, and National Weather Service (DMC) in Temuco, Osorno and Melinka for taking care of the weather stations installed during this research.

REFERENCES

Austin, R. T., A. J. Heymsfield, and G. L. Stephens (2009), Retrieval of ice cloud microphysical parameters using the CloudSat millimeter-wave radar and temperature, *J. Geophys. Res. Atmos.*, 114, D00A23, doi:10.1029/2008JD010049.

Barrett, B. S., R. D. Garreaud, and M. Falvey (2009), Effect of the Andes Cordillera on precipitation from a midlatitude cold front, *Mon. Wea. Rev.*, 137, 3092–3109.

Castro, L. M., J. Gironás, B. Fernández (2014), Spatial estimation of daily precipitation in regions with complex relief and scarce data using terrain orientation, *Journal of Hydrology*, 517, 481-492.

Daly, C., R. P. Neilson, D. L. Phillips (1994), A statistical-topographic model for mapping climatological precipitation over mountainous terrain, *J. Appl. Meteorol.*, 33 (2), 140–158.

Falvey, M., and R. Garreaud (2007), Wintertime precipitation episodes in Central Chile: associated meteorological conditions and orographic influences, *J. Hydrometeor.*, 8, 171-193.

Garreaud, R. D., P. Lopez, M. Minvielle, and M. Rojas (2013), Large-scale control on the Patagonian climate, *J. Climate*, 26, 215–230.

Garreaud, R. D., M. G. Nicora, R. E. Bürgesser, and E. E. Ávila (2014), Lightning in Western Patagonia, *J. Geophys. Res. Atmos.*, 119, 4471–4485, doi:10.1002/2013JD021160.

Houze, R. A. Jr. (1993), Cloud Dynamics. Academic Press, San Diego, Calif.

Houze, R. A. Jr. (2012), Orographic effects on precipitating clouds. *Rev. Geophys.*, 50, RG1001, doi:10.1029/2011RG000365.

Im, E., C.L. Wu, and S.L. Durden (2005), Cloud profiling radar for CloudSat mission, *IIEE Aerosp. Electron. Syst. Mag.*, 20, 15-18.

Lenaerts, J., M. Van den Broeke, J. Van Wessem, W. Van de Berg, E. Van Meijgaard, L. Van Ulft, and M. Schaefer (2014), Extreme precipitation and climate gradients in Patagonia revealed by high-resolution regional atmospheric climate modelling, *J. Climate*, 27, 4607–4621.

Mace, G. G., Q. Zhang, M. Vaughan, R. Marchand, G. Stephens, C. Trepte, and D. Winker (2009), A description of hydrometeor layer occurrence statistics derived from the first year of merged Cloudsat and CALIPSO data, *J. Geophys. Res. Atmos.*, 114, doi:10.1029/2007JD009755.

Matrosov, S. Y. (2013), Characteristics of landfalling atmospheric rivers inferred from satellite observations over the eastern North Pacific Ocean, *Mon. Wea. Rev.*, 141, 3757–3768.

Smith, R. B., and J. P. Evans (2007), Orographic precipitation and isotope fraction over the southern Andes, *J. Hydrometeor.* , 8, 3-14.

Stephens, G. L., and coauthors (2002), The CloudSat mission and the A-train. A new dimension of space-based observations of clouds and precipitation, *Bull. Am. Meteorol. Soc.*, 83, 1771-1790.

Viale, M., and M. N. Nuñez (2011), Climatology of winter orographic precipitation over the Subtropical Central Andes and associated synoptic and regional characteristics, *J. Hydrometeor.*, 12, 481-507.

Viale, M., R. A. Jr. Houze,, and K. L. Rasmussen (2013), Upstream orographic enhancement of a narrow coldfrontal rainband approaching the Andes, *Mon. Wea. Rev.*, 141, 1708–1730.

Winker, D.M., M. A. Vaughan, A. H. Omar, Y. Hu, K. A. Powell, Z. Liu, W. H.Hunt, and S. A. Young (2009), Overviewof the CALIPSO mission and CALIOP data processing algorithms, *J. Atmos. Oceanic Technol.*, 26, 2310–2323.